Hadron Propagation in Medium: the Exclusive Process A(e,e'p)B in Few-Nucleon Systems

C. Ciofi degli Atti[a], L. P. Kaptari[a*] and H. Morita[a†]

[a]Department of Physics, University of Perugia and Istituto Nazionale di Fisica Nucleare, Sezione di Perugia, Via A. Pascoli, I-06123, Italy

The mechanism of propagation of hadronic states in the medium is a key point for understanding particle-nucleus and nucleus-nucleus scattering at high energies. We have investigated the propagation of a baryon in the exclusive process A(e,e'p)B in few-nucleon systems using realistic nuclear wave functions and Glauber multiple scattering theory both in its original form and within a generalized eikonal approximation. New results for the processes $^3He(e,e'p)^2H$ and $^4He(e,e'p)^3H$ are compared with data recently obtained at the Thomas Jefferson Laboratory (JLAB).

1. Introduction

Exclusive and semi-inclusive lepton scattering off nuclei $A(l,l'p)X$ in the quasi elastic region, plays a relevant role in nowadays hadronic physics, mainly for three reasons: i) due to the wide kinematical range available by present experimental facilities non trivial information on nuclei (e.g. nucleon-nucleon (NN) correlations) can be obtained; ii) the mechanism of propagation of hadronic states can be investigated in great details; iii) at high energies color transparency effects might be investigated. The key point here is a reliable evaluation of the mechanisms of propagation of the produced hadrons in the medium, a task which is usually referred to as the problem of the evaluation of the Final State Interaction (FSI). At medium and high energies hadron propagation is usually treated within the Glauber multiple scattering approach (GA) , which has been applied with great success to hadron scattering off nuclear targets [1]. However, when the hadron is created inside the nucleus, as in a process $A(l,l'p)X$, various improvements of the original GA have been advocated. Most of them are based upon a Feynman diagram reformulation of GA; such a diagrammatic approach, has been developed long ago for the case of hadron-nucleus scattering [2] and it has been generalized to the process $A(l,l'p)X$ [3, 4], showing that in particular kinematical regions it predicts appreciable deviation from GA. In such an approach, based upon a generalized eikonal approximation (GEA) the frozen approximation, common to GA, is partly removed by taking into account the excitation energy of the $A-1$ system, which results in a correction term to the standard profile function of GA, leading to an additional contribution to the longitudinal component of the

*On leave from Bogoliubov Lab. Theor. Phys., 141980, JINR, Dubna, Russia

†On leave from Faculty of Social Information, Sapporo Gakuin University, 11 Bunkyo-dai, Ebetsu-shi, Hokkaido 069-8555, Japan

missing momentum. The GEA has recently been applied to a systematic calculation of the exclusive processes $^3He(e,e'p)^2H$ and $^3He(e,e'p)(np)$ [5, 6] using realistic three-body wave functions [7] and two-nucleon interactions (AV18) [8]; the results of calculations show a nice agreement with recent Thomas Jefferson Laboratory (JLAB) data [9]. The two-body break up channel $^3He(e,e'p)^2H$ has also been considered within the Glauber approach in [10], obtaining results consistent with Ref. [5, 6]. The aim of this contribution is twofold: i) to extend the GEA calculation to the four-body system, namely to the calculation of the process $^4He(e,e'p)^3H$, for which recent data have been obtained at JLAB [11]; ii) to consider for the same reaction, through the concept of Finite Formation Time (FFT) as developed in Ref. [13], the role played by nucleon virtuality which is expected to become important at high values of Q^2. Our paper is organized as follows: in Section 2 the basic elements of our theoretical framework are given; the comparison of our results with experimental data on $^3He(e,e'p)^2H(pn)$ and $^4He(e,e'p)^3H$ reactions are presented in Section 3; FFT effects on the process $^4He(e,e'p)^3H$ are illustrated in Section 4; the Summary and Conclusions are given in Section 5.

2. The cross section for the process A(e,e'p)B within GA and GEA

The FSI which is considered in the diagrammatic approach of Ref. [3, 4, 5, 6] is the elastic scattering of the hit nucleon by the nucleons of the spectator $A-1$. Under two main assumptions which are expected to be valid at medium and high energies, namely that: i) in each rescattering process the momentum transfer is small, and ii) the spin flip part of the NN scattering amplitude can be disregarded, the method predicts that nuclear effects in the exclusive process $A(e,e'p)B$ should be governed by the Distorted Spectral Function

$$P_A^{FSI}(\mathbf{p}_m,E_m) = \frac{1}{(2\pi)^3}\frac{1}{2J_A+1}\sum_f \sum_{\mathcal{M}_A,\mathcal{M}_{A-1},\,s_1}\left|\sum_{n=0}^{A-1}\mathcal{T}_A^{(n)}(\mathcal{M}_A,\mathcal{M}_{A-1},s_1;f)\right|^2 \times \\ \times\ \delta\left(E_m-(E_{A-1}^f+E_{min})\right) \quad (1)$$

where $\mathbf{p}_m=\mathbf{P_{A-1}}=\mathbf{q}-\mathbf{p}_1$ and $E_m=E_{min}+E_{A-1}^f$ are the *missing momentum* and *missing energy*, respectively (here $\mathbf{p}_1$ and $\mathbf{q}$ are the momentum of the detected nucleon and the 3-momentum transfer, respectively, and $E_{min}=E_A-E_{A-1}$, E_A and E_{A-1} being the positive ground state energies of A and $A-1$); $\mathcal{M}_A$, $\mathcal{M}_{A-1}$, and s_1, are magnetic quantum numbers; the sum over f stands for a sum over all possible discrete and continuum states of the $A-1$ system; $\mathcal{T}_A^{(n)}$ represents the the reduced (Lorentz index independent) amplitude which, at order n, takes into account all possible diagrams describing n-body rescattering (see [5]). After the evaluation of all single and double scattering diagrams, the distorted spectral function of ^3He reads as follows

$$P_3^{FSI}(\mathbf{p}_m,E_m)=\frac{1}{2(2\pi)^3}\sum_{f=D,np}\sum_{\mathcal{M}_3,\mathcal{M}_2,s_1}\left|\int e^{i\boldsymbol{\rho}\cdot\mathbf{p}_m}\chi^\dagger_{\frac{1}{2}s_1}\Psi_f^{\mathcal{M}_2\,\dagger}(\mathbf{r})\mathcal{S}_{GEA}(\boldsymbol{\rho},\mathbf{r})\Psi_{He}^{\mathcal{M}_3}(\boldsymbol{\rho},\mathbf{r})d\boldsymbol{\rho}d\mathbf{r}\right|^2 \times \\ \times\ \delta\left(E_m-(E_{A-1}^f+E_{min})\right) \quad (2)$$

where $E^f_{A-1} + E_{min} = E_{min}$, for the two-body break up (2buu) channel ($f = D$), and $E^f_{A-1} + E_{min} = \mathbf{t}^2/M_N + E_3$, for the three-body break up (3buu) ($f = (np)$) channel (here $\mathbf{t}$ is the relative momentum of the interacting $(n-p)$ pair in the continuum. The quantity $\mathcal{S}_{GEA}$ introduces FSI and has the form $\mathcal{S}_{GEA} = \mathcal{S}^{(1)}_{GEA} + \mathcal{S}^{(2)}_{GEA}$, with

$$\mathcal{S}^{(1)}_{GEA}(\boldsymbol{\rho}, \mathbf{r}) = 1 - \sum_{i=2}^{3} \theta(z_i - z_1) \mathrm{e}^{i\Delta_z(z_i - z_1)} \Gamma(\mathbf{b}_1 - \mathbf{b}_i) \tag{3}$$

and

$$\begin{aligned} \mathcal{S}^{(2)}_{GEA}(\boldsymbol{\rho}, \mathbf{r}) &= \Big[\theta(z_2 - z_1)\theta(z_3 - z_2)\mathrm{e}^{-i\Delta_3(z_2 - z_1)}\mathrm{e}^{-i(\Delta_3 + \Delta_z)(z_3 + z_1)} + \\ &+ \theta(z_3 - z_1)\theta(z_2 - z_3)\mathrm{e}^{-i\Delta_2(z_3 - z_1)}\mathrm{e}^{-i(\Delta_2 + \Delta_z)(z_2 - z_1)}\Big] \Gamma(\mathbf{b}_1 - \mathbf{b}_2)\Gamma(\mathbf{b}_1 - \mathbf{b}_3) \end{aligned} \tag{4}$$

where $\Delta_i = (q_0/|\mathbf{q}|)(E_{\mathbf{k}_i} - E_{\mathbf{k}'_i})$ and $\Delta_z = (q_0/|\mathbf{q}|)E_m$, $\mathbf{k}_i$, $\mathbf{k}'_i$, being nucleon momenta before and after the rescattering. It can be seen that Δ_z takes into account Fermi motion and therefore partly remove the frozen approximation. Note that when $\Delta_i = \Delta_z = 0$, the usual GA is recovered.

3. Calculations of the processes $^3He(e,e'p)^2H(pn)$ and $^4He(e,e'p)^3H$ Reaction

Within the diagrammatic approach, the differential cross section assumes a factorized form, namely

$$\frac{d^6\sigma}{d\nu d\Omega_e dp d\Omega_p} = \mathcal{K}\sigma_{ep} P^{FSI}_A(\mathbf{p}_m, E_m), \tag{5}$$

where $\mathcal{K}$ is a kinematical factor, σ_{ep} the electron-nucleon cross section and ν the energy transfer. We have calculated the cross sections of the processes $^3He(e,e'p)^2H$, $^3He(e,e'p)(np)$, and $^4He(e,e'p)^3H$ using the well known parametrization of the profile function

$$\Gamma(\mathbf{b}) = \frac{\sigma^{tot}_{NN}(1 - i\alpha_{NN})}{4\pi b_0^2}\, e^{-\mathbf{b}^2/2b_0^2} \tag{6}$$

with all parameters taken from Ref. [12]. For the electron-nucleon cross section σ_{ep} we used the De Forest $\sigma^{cc1}_{ep}(\bar{Q}^2, \mathbf{p}_m)$ cross section [15]. All two-, three-, and four-body wave functions are direct solutions of the non relativistic Schrödinger equation, therefore our calculations are fully parameter free.

In case of the three-nucleon system, the results for the 2bbu and 3bbu channels are shown in Figs. 1 and 2 [6]. The missing momentum dependence of the experimental cross section clearly exhibits different slopes, that are reminiscent of the slopes observed in elastic hadron-nucleus scattering at intermediate energies (see e.g. Ref. [1]) and our parameter free calculations demonstrate that: i) these slopes are indeed related to multiple scattering in the final state, and ii) a highly satisfactory agreement between theory and experiment is obtained, which means that in the energy-momentum range covered by the data, FSI can be described by elastic rescattering; iii) GA and GEA, differ only by a few percent.

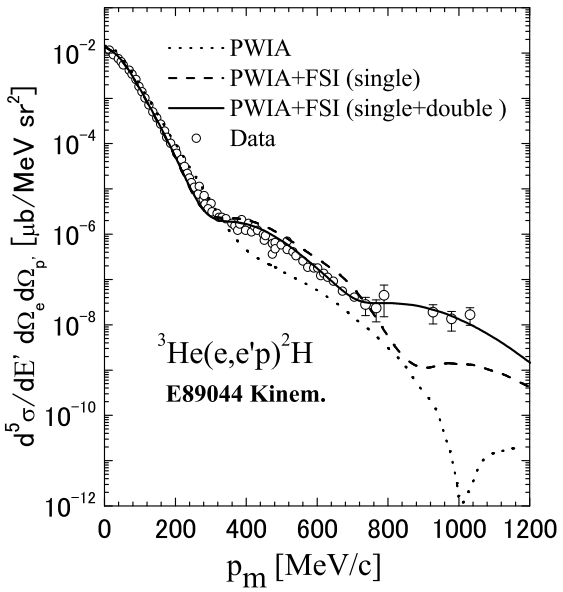

Figure 1. Results for the $^3He(e,e'p)^2H$ reaction [6]. Dotted curve: PWIA result; dashed curve: FSI (single rescattering); solid curve: FSI (single plus double rescattering). Experimental data from [9].

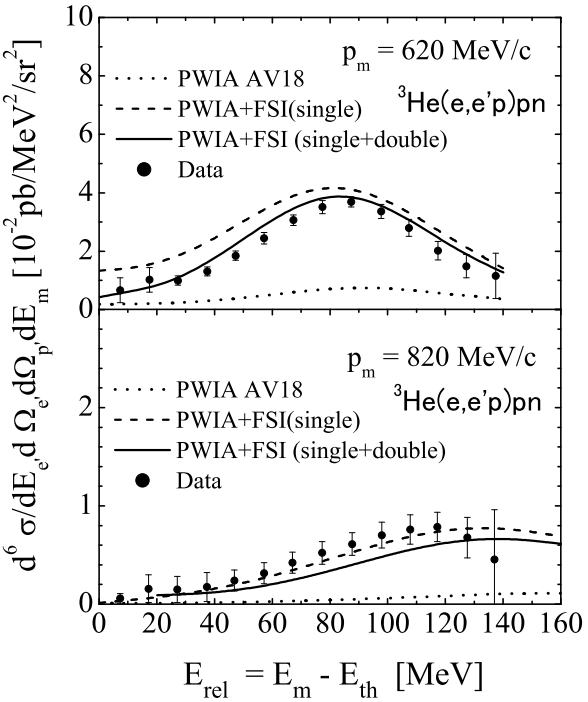

Figure 2. The same as in Fig. 1 but for the process $^3He(e,e'p)pn$ ($E_{th} = E_3$ is the two-nucleon emission threshold in ^3He).

The results for ^4He, for which $\mathcal{S}_{GEA} = \mathcal{S}^{(1)}_{GEA} + \mathcal{S}^{(2)}_{GEA} + \mathcal{S}^{(3)}_{GEA}$, are presented for the first time in Figs. 3 and 4. In this case, we have used realistic variational wave functions for both ^4He and ^3H [16, 17], corresponding to the RSC V8 model potential[18]. Calculations for the reduced cross section

$$n_D(\mathbf{p}_m) = \frac{d^5\sigma}{d\omega d\Omega_e d\Omega_p}(\mathcal{K}\sigma_{ep})^{-1}, \tag{7}$$

are compared with the JLab E97111 experimental data in parallel(Py2) and perpendicular (CQω2) kinematics [11]. Fig. 3 shows that: i) the dip predicted by the PWIA is totaly filled up by the FSI; ii) like the ^3He case, the difference between GA and GEA is very small; iii) although we predict an overall satisfactory behaviour of the experimental data in parallel kinematics, we systematically underestimate them. In case of perpendicular kinematics, shown in Fig. 4, the agreement between theory and experiment is much better and the differences between GA and GEA are more pronounced. The multiple scattering contributions are illustrated in Fig. 5. As the case of ^3He the single rescattering amplitude dominates at $p_m \leq 600\, MeV/c$ whereas at higher values of p_m multiple scattering effects become important, with the triple rescattering term contributing significantly at $p_m > 800\, MeV/c$. In our calculations we have always directed the z-axis along the momentum of the propagating nucleon $\mathbf{p}_1$. In several Glauber-type calculations the z-axis is chosen along q, assuming $|\mathbf{q}|$ to be large enough. Fig. 6 shows that this is not the case in the JLAB kinematics, with the calculation with the z-axis directed along $\mathbf{q}$ underestimating the correct results by a large factor.

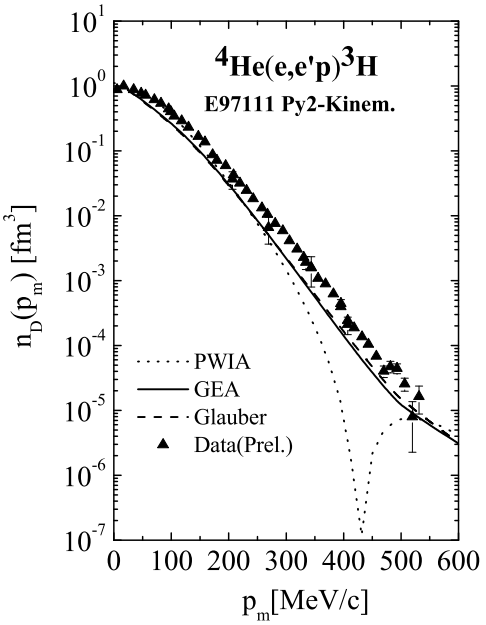

Figure 3. The reduced cross section $n_D(\mathbf{p}_m) = [d^5\sigma/(d\nu d\Omega_e d\Omega_p)] \times [\mathcal{K}\sigma_{ep}]^{-1}$ for the process $^4He(e,e'p)^3H$ in parallel kinematics. Preliminary data from [11].

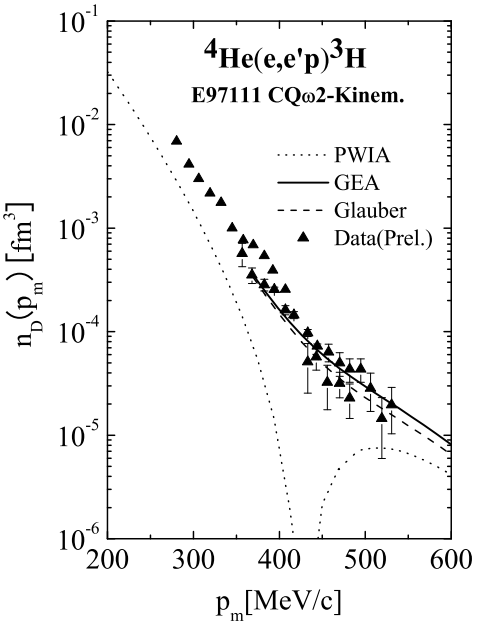

Figure 4. The same as in Fig. 3 but for perpendicular kinematics.

4. Finite Formation Time Effects in the process $^4He(e,e'p)^3H$

It has been argued by various authors that at high values of Q^2 the phenomenon of color transparency, i.e. a reduced NN cross section in the medium, might be observed. Color transparency is a consequence of the cancelation between various hadronic intermediate states of the produced ejectile. In [13] the vanishing of FSI at Q^2 has been produced by considering the finite formation time (FFT) the ejectile needs to reach its asymptotic form of a physical baryon. This has been implemented by explicitly considering the virtuality dependence of the NN scattering amplitude. According to [13] FFT effects can be introduced in Eq. (2) by replacing $\mathcal{S}_{GEA}$ with $\mathcal{S}_{FFT}$, which is obtained from $\mathcal{S}_{GEA}$ simply by letting $\Delta_i = \Delta_z = 0$ and replacing $\theta(z_i - z_1)$ by

$$J(z_i - z_1) = \theta(z_i - z_1)\left(1 - \exp[-(z_i - z_1)/l(Q^2)]\right) \tag{8}$$

with $l(Q^2) = Q^2/(x m_N M^2)$ where x is the Bjorken scaling variable and the quantity $l(Q^2)$ plays the role of the proton formation length, the length of the trajectory that the knocked out proton runs until it return to its asymptotic form. The quantity M is related to the nucleon massm_N and to an average resonance state of mass m^* by $M^2 = m^{*2} - m_N^2$; the value $m^* = 1.8$ GeV has been used in the calculations[13]. Since this formation length grows linearly with Q^2, at higher Q^2 the strength of the Glauber-type FSI is reduced by the damping factor $(1-\exp[-(z_i-z_1)/l(Q^2)])$ appearing in Eq. (8), which physically describes the following situation: once the hit proton virtually reaches a resonance state, it will need

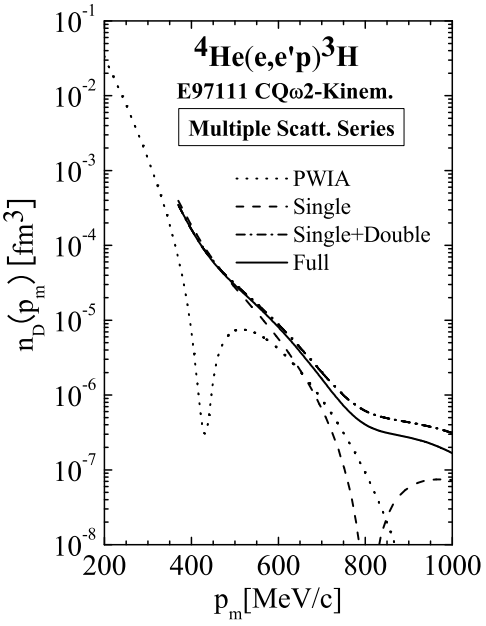

Figure 5. Multiple scattering contributions in the process $^4He(e,e'p)^3H$. The results are similar to the ones shown in Fig. 1, but in this case triple rescattering contributions start to contribute at $p_m \geq 800\,MeV/c$.

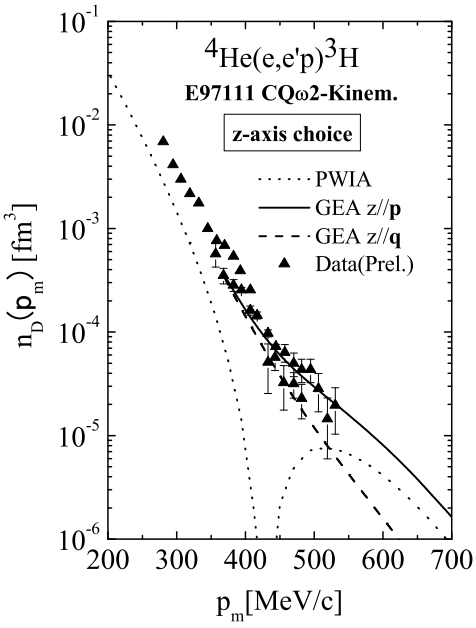

Figure 6. The choice of z-axis for the Glauber operator. The dashed curve corresponds to the calculation with the z-axis along the direction of $\mathbf{q}$. See text. Preliminary data from [11]

a finite amount of time to return to its asymptotic form, during which FSI becomes weaker than the Glauber one; if $l(Q^2) = 0$, then S_{FFT} reduces to the usual Glauber operator S_G. We have calculated the cross section of the process $^4He(e,e'p)^3H$ in perpendicular kinematics introducing FFT effects (see also [14]). The results are presented in Figs. 7 and 8. It can be seen that at the JLAB kinematics ($Q^2 = 1.78\,(GeV/c)^2$, $x \sim 1.8$) FFT effects, as expected, are too small to be detected. We have therefore extended our calculation to higher values of Q^2 reducing the value of x to x =1.4 (in the $CQ\omega 2$ kinematics the region with $p_m < 500\,MeV/c$ and $Q^2 \geq 5\,(GeV/c)^2$ is kinematically forbidden at $x = 1.8$). The results, presented in Fig. 8, show that FFT effects could unambiguously be detected in the region $5 \leq Q^2 \leq 10\,(GeV/c)^2$. Thus, observing the Q^2 dependence of the cross section of $^4He(e,e'p)^3H$ process at $p_m \sim 430\,MeV/c$ region up to around $Q^2 \sim 10\,(GeV/c)^2$ would be of of great interest.

5. Summary and Conclusions

We have performed a realistic calculation of the cross section of the processes $^3He(e,e'p)^2H$, $^3He(e,e'p)(np)$ and $^4He(e,e'p)^3H$, using few-body wave functions which exhibit the very rich correlation structure generated by modern NN interactions and describing the propagation of the hit nucleon in the medium in term of elastic rescattering; to this end we have used the standard Glauber approximation (GA), as well as its generalized version (GEA). The two approaches differ in that the latter takes into account in the NN scatter-

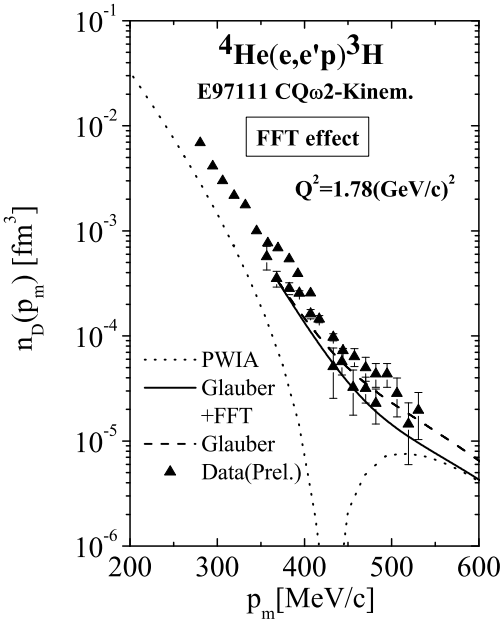

Figure 7. The FFT effect on the CQω2 kinematics. The solid line shows the results within GEA, whereas the dashed curve corresponds to the conventional GA. Preliminary data from [11].

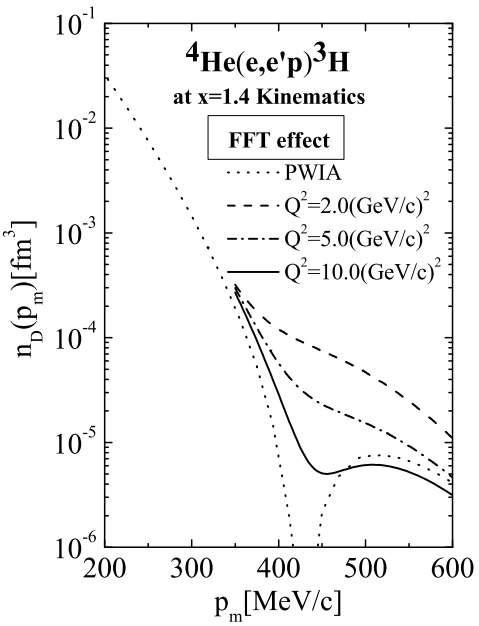

Figure 8. The Q^2 dependence of FFT effects at perpendicular kinematics with x=1.4.

ing amplitude the removal energy of the struck nucleon, or, equivalently, the excitation energy of the system $A-1$. Our approach is a very transparent one and fully parameter free.

The main results we have obtained, can be summarized as follows: i) the agreement between the results of our calculations and the experimental data for both ^3He and ^4He, is a very satisfactory one, particularly in view of the lack of any adjustable parameter in our approach; ii) the effects of the FSI are such that they systematically bring theoretical calculations in better agreement with the experimental data; for some quantities, they simply improve the agreement between theory and experiment, whereas for some other quantities, they play a dominant role; iii) the 3bbu channel in ^3He, i.e. the process $^3He(e,e'p)(np)$, provides evidence of NN correlations, in that the experimental values of p_m and E_m corresponding to the maximum values of the cross section, satisfy to a large extent the relation predicted by the two-nucleon correlation mechanism namely $E_m \simeq p_m^2/4M_N + E_3$, with the full FSI mainly affecting only the magnitude of the cross section; iv) both for ^3He and ^4He the p_m dependence of the cross section exhibits peculiar slopes which can be interpreted in terms of multiple scattering effects, with triple scattering in ^4He starting to significantly contribute at $p_m \geq 800\, MeV/c$. v) in the kinematical range we have considered only minor numerical differences were found between the conventional Glauber-eikonal approach and its generalized extension; vi) finally, we investigated the Finite Formation Time effects, which weakens the FSI at high

Q^2; we found that available data on the $^4He(e,e'p)^3H$ process are only slightly affected by FFT effects, but, at the same time, similar data at $Q^2 \geq 2(GeV/c)^2$ in the dip region ($p_m \simeq 430\, MeV/c$) would provide a significant check of theoretical models of FFT effects.

Final results of our calculations, including also a quantitative investigation of the limits of validity of the factorized cross section, will be presented elsewhere [19].

6. Acknowledgments

L.P.K. and H.M. are indebted to the University of Perugia and INFN, Sezione di Perugia, for support and hospitality.

REFERENCES

1. R. J. Glauber, in *High Energy Physics and Nuclear Structure*, p.207, S. Devons Ed., NY Plenum Press (1970).
2. V.N.Gribov, Sov. Phys. JETP, **30** (1970) 709.
3. L.L. Frankfurt, M.M. Sargsian and M.I. Strikman Phys. Rev. C56(1997) 1124.
4. M.M. Sargsian, T.V. Abrahamyan, M.I. Strikmn and L.L. Frankfurt, Phys. Rev. C71(2005)044614.
5. C. Ciofi degli Atti and L.P. Kaptari, Phys. Rev. C71 (2005) 024005.
6. C. Ciofi degli Atti and L.P. Kaptari, Phys. Rev. Lett. 95 (2005) 052502.
7. A. Kievsky , S. Rosati and M. Viviani, Nucl. Phys. A551(1993)241; A. Kievsky, *Private communication*.
8. R.B. Wiringa, V.G. Stokes and R. Schiavilla, Pys. Rev. C51 (1995) 38.
9. F. Benmokhtar et al., Phys. Rev. Lett. 94(2005)082325.
10. R. Schiavilla et al.Phys. Rev. C72(2005)064003
11. B. Reitz et al., Eur. Phys. J. A S19(2004)165.
12. http://pdg.lbl.gov and http://lux2.phys.va.gwu.edu.
13. M.A. Braun, C. Ciofi degli Atti and D. Treleani, Phys. Rev. C62(2000)034606.
14. H. Morita, M. Braun, C. Ciofi degli Atti and D. Treleani, Nucl. Phys. A699(2002)328c.
15. T. De Forest, Jr., Nucl. Phys. A392(1983)232.
16. M. Sakai, I. Shimodaya, Y. Akaishi, J. Hiura and H. Tanaka, Prog. Theor. Phys. Suppl. 56(1974)32.
17. H. Morita, Y. Akaishi, O. Endo and H. Tanaka, Prog. Theor. Phys. 78(1987)1117; H. Morita, Y. Akaishi and H. Tanaka, Prog. Theor. Phys. 79(1988)1279.
18. I.E. Largaris and V.R. Pandharipande, Nucl. Phys. A359(1981)331.
19. C. Ciofi degli Atti, L. P. Kaptari and H. Morita, to appear.

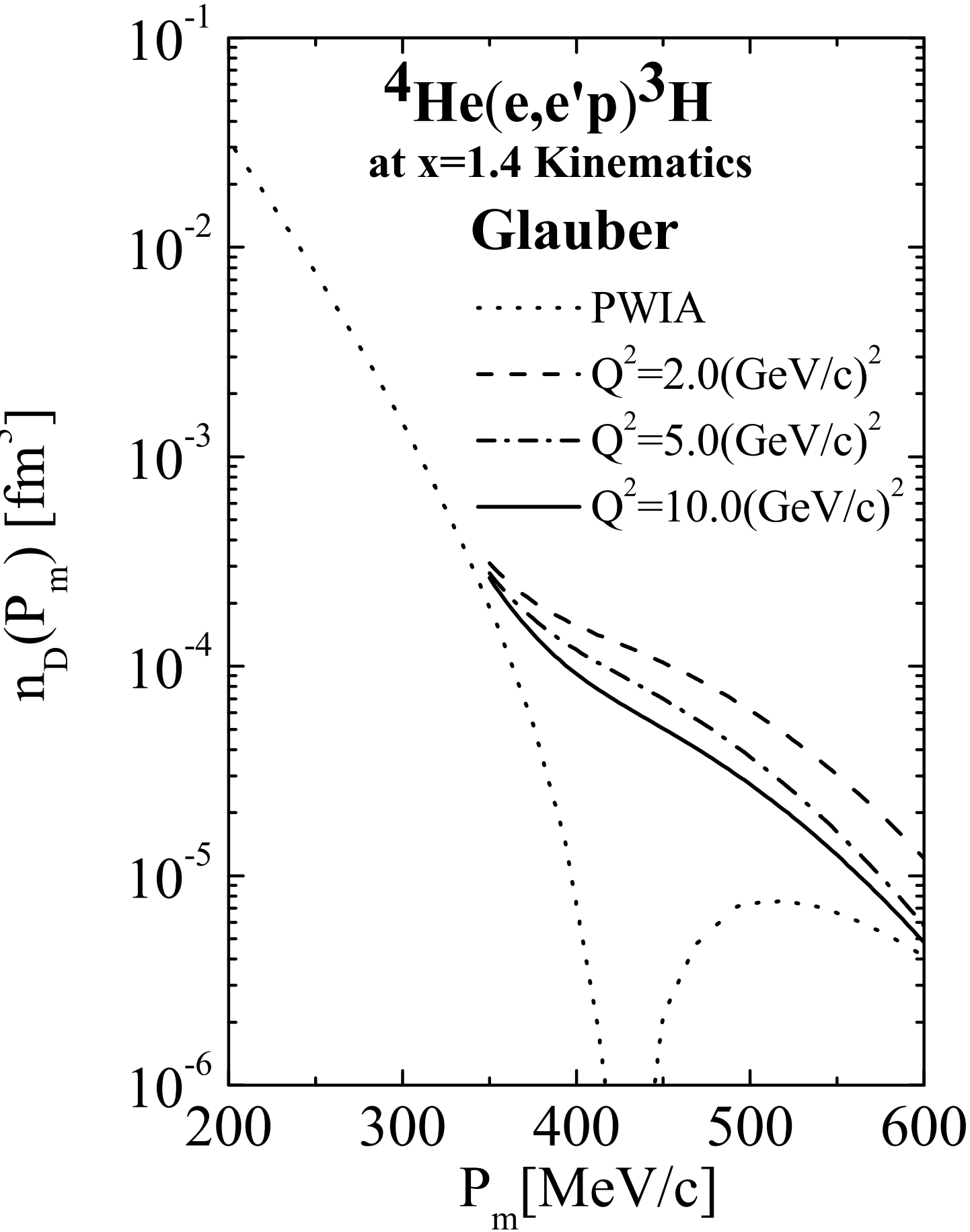
^{4}He(e,e'p)^{3}H
at x=1.4 Kinematics
Glauber
PWIA
Q^2=2.0(GeV/c)^2
Q^2=5.0(GeV/c)^2
Q^2=10.0(GeV/c)^2
$n_D(P_m)$ [fm^3]
P_m[MeV/c]
10^{-1}
10^{-2}
10^{-3}
10^{-4}
10^{-5}
10^{-6}
200
300
400
500
600